Influence of Osmolytes on *In Vivo* Glucose Monitoring Using Optical Coherence Tomography

VERONIKA V. SAPOZHNIKOVA,* DONALD PROUGH,† ROMAN V. KURANOV,* INGA CICENAITE,* AND RINAT O. ESENALIEV,*,†,‡,[1]

Laboratory for Optical Sensing and Monitoring, Center for Biomedical Engineering, †Department of Anesthesiology, and ‡Department of Neuroscience and Cell Biology, University of Texas Medical Branch, Galveston, TX 77555-0456

Diabetes mellitus and its complications are the third leading cause of death in the world, exceeded only by cardiovascular disease and cancer. Tighter monitoring and control of blood glucose could minimize complications associated with diabetes. Recently, optical coherence tomography (OCT) for noninvasive glucose monitoring was proposed and tested *in vivo*. The aim of this work was to investigate the influence of changes in blood glucose concentration ([glu]) and sodium concentration ($[Na^+]$) on the OCT signal. We also investigated the influence of other important analytes on the sensitivity of glucose monitoring with OCT. The experiments were carried out in anesthetized female pigs. The OCT images were acquired continuously from skin, while [glu] and $[Na^+]$ were experimentally varied within their physiological ranges. Correlations of the OCT signal slope with [glu] and $[Na^+]$ were studied at different tissue depths. The tissue area probed with OCT was marked and cut for histological examination. The correlation of blood [glu] and $[Na^+]$ with the OCT signal slope was observed in separate tissue layers. On average, equimolar changes in [glu] produced 2.26 ± 1.15 greater alterations of the OCT signal slope than changes in $[Na^+]$. Variation of concentrations of other analytes did not influence the OCT signal slope. The influence of $[Na^+]$ on relative changes in the OCT signal slope was generally less than [glu]-induced changes. OCT is a promising method for noninvasive glucose monitoring because of its ability to track the influence of changing [glu] on individual tissue layers. Exp Biol Med 231:1323–1332, 2006

This study was supported by grant R01 EB001467 from the National Institute for Biomedical Imaging and Bioengineering, National Institutes of Health.

[1] To whom correspondence should be addressed at Laboratory for Optical Sensing and Monitoring, Center for Biomedical Engineering, University of Texas Medical Branch, 301 University Blvd., Rt. 0456, Galveston, TX 77555-0456. E-mail: riesenal@utmb.edu

Received October 4, 2005.
Accepted March 18, 2006.

1535-3702/06/2318-1323$15.00

Key words: diabetes; glucose monitoring; optical coherence tomography

Introduction

Currently, only cardiovascular disease and cancer cause more deaths than diabetes mellitus. As many as 120–180 million people, or 2%–3% of the world population, suffer from diabetes (1, 2). In patients with diabetes, effective control of blood glucose concentration ([glu]) limits the complications of the disease. Current monitoring of [glu] requires blood sampling, which discourages frequent glucose measurement and tight control. Thus, the development of efficient and reliable noninvasive sensors for [glu] monitoring would improve the management of diabetes.

At the present time, two types of glucose sensors are under development: minimally invasive and noninvasive. Minimally invasive sensors are based on analysis of tissue interstitial fluid. Most of the noninvasive methods use optical signals (2–4). One of them, optical coherence tomography (OCT), is a promising technique for blood [glu] monitoring (5–7).

OCT, a nondestructive technique that examines the internal structure of superficial layers of biological tissues, is based on interferometric recording of near-infrared light backscattered from the object. Backscattered light is collected, measured, and integrated to assemble an image. Initially, OCT was successfully applied to imaging alterations in ocular tissues (8, 9). Subsequently, OCT has been widely used in medical studies for high-resolution visualization of the internal structures of the superficial layers of epithelial tissues in humans and animals (10–12). Many pathological processes, such as dysplasia and cancer, alter the typical layered structure of healthy tissue, and these changes can be detected by OCT (13). High-resolution OCT imaging techniques can ensure *in vivo* observation (monitoring) of the state of internal tissue structures in humans and animals (14).

Previous studies have quantified alterations in the optical parameters of tissues produced by changes in hydration (15) and temperature (16, 17) and by the addition of chemical agents (18–20). Variations of these factors produced changes in the light-scattering properties of tissues. Likewise, increases in blood [glu] decreased the total light-scattering coefficient in tissues as a consequence of better refractive index matching between intracellular and extracellular components (3).

Recent *in vivo* and *in vitro* experiments demonstrated that OCT detects tissue changes induced by variation of [glu] within the usual pathophysiological range (3–30 m*M*; 54–540 mg/dl; Refs. 5–7). Normal fasting blood [glu] is less than 110 mg/dl, with increases to 150–180 mg/dl shortly after eating. In critically ill patients, the maintenance of [glu] at 80–110 mg/dl was associated with improved mortality in comparison with those with wider [glu] fluctuation (21). Previous *in vivo* studies illustrated that the slope of the OCT signal strongly correlates with [glu] when the probing beam is scanned laterally over a straight line (5, 6). It was also reported in a pilot study that changes in blood pressure, heart rate, hematocrit (Hct), surgical procedure, and anesthesia did not influence the correlation of the OCT signal slope with blood [glu] (7). Equally important, theoretical calculations were confirmed *in vitro* that suggest that changes in the refractive index produced by changes in [glu] considerably exceed changes in the refractive index produced by changes in other analyte concentrations within the physiological range (22). However, *in vivo* changes in the concentrations of other analytes, especially the concentration of sodium ($[Na^+]$), may sufficiently alter osmolality so that the hydration of individual tissue layers may change. The associated changes in backscattering produced by these osmotic effects could also influence measurements of [glu].

In the present study, we investigated the influence of large acute changes in blood [glu] on the OCT signal *in vivo* and the influence of large acute changes in $[Na^+]$. We also studied the influence of other agents such as $[Cl^-]$, $[K^+]$, and urea on measurement of blood [glu] using OCT.

Materials and Methods

In these experiments, we used the OCT device described in detail in previous publications. In those studies, the OCT setup was used in a one-dimensional (1-D) scanning mode, in which the probing beam was scanned laterally over a straight line (5–7). However, 1-D scanning is sensitive to motion artifacts and generates a high level of speckle noise. It was previously shown that two-dimensional (2-D) lateral scanning of the OCT probing beam significantly reduced speckle noise, thereby reducing uncertainty in the OCT signal measurements (23). In addition, the 2-D scanning mode is less sensitive to motion artifacts because the scanned area of 600 × 600 μm is 50-fold greater than that of the 1-D mode. The acquisition time for one 2-D mode OCT image comprising 1800 independent A-scans (depth profiles) was about 30 secs.

We studied 13 young (age, 3–4 mos) female pigs weighing 20–25 kg. In seven pigs, we intravenously injected 7.7% saline (NaCl) solution ($[Na^+]$ 1317 mEq/l; normal blood $[Na^+]$ ~ 40 mEq/l), followed at least 40–60 mins later by injection of 50% glucose solution (50% dextrose; Abbot Laboratories, North Chicago, IL) intravenously ([glu] 50 g/dl; normal blood [glu] ~100 mg/dl). In two pigs, we injected glucose first, followed at least 40–60 mins later by 7.7% NaCl. Of the remaining four pigs, one served as a control (no injections), two received only 7.7% NaCl, and one received only glucose.

The OCT images were obtained from the skin in the abdominal area and were converted into the OCT signals by averaging the in-depth (*z*-axial) scans. The OCT signals in logarithmic scale were used in subsequent calculations of the OCT signal slopes. The 2-D lateral (*x* and *y*) scanning mode of the OCT probe beam was used to calculate the OCT signal slopes at different depths. The OCT signal slope was calculated using least squares linear approximation of the OCT signal segment with a length of 70 ± 20 μm: $y = ax + b$, where *a* and *b* are coefficients of linear regression and *a* was used for estimation of the OCT signal slope value (Fig. 1). The length of approximated segments was roughly equal to the half-distance between collagen bundles in skin, which varied among pigs and occasionally within a single pig. The distance between collagen bundles was verified by standard hematoxylin-eosin (H&E) histology. In every pig, we calculated dependence of the OCT signal slope versus time in the segments with a step 20–40 μm (segments overlapped) from the epidermis and to the dermis-

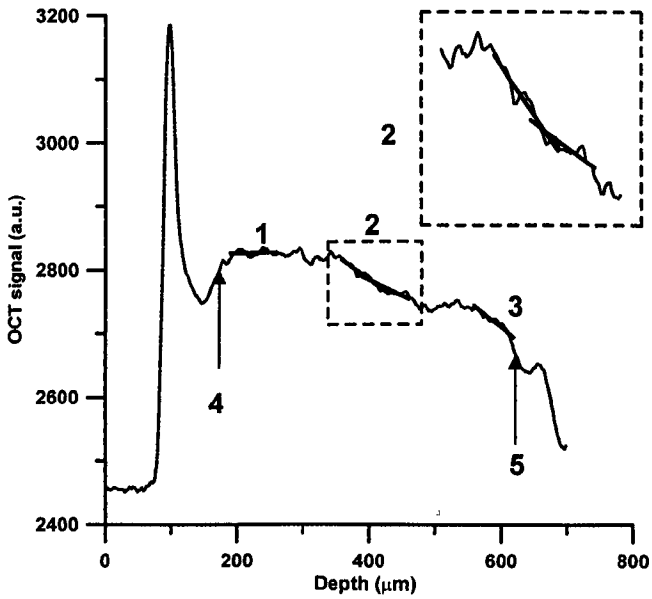

Figure 1. Typical OCT signal averaged more than 1800 independent A-scans versus geometrical depth. (1), initial; (2), two neighbor; (3), last fits over 70-μm segments that were used to calculate the OCT signal slope; (4), papillary-reticular junction; and (5), dermis-hypodermis junction.

hypodermis junction. We analyzed changes in the OCT signal slope versus time and calculated the correlation coefficient (R) between the OCT signal slope and blood [glu]. For calculating the correlation coefficient, we smoothed the OCT signal slope versus time using Fourier filtration technique. We calculated the correlation coefficient at different time delays between the OCT signal slope and blood [glu]. We considered that the correlation between the OCT signal slope and [glu] was absent if the absolute value of the correlation coefficient ($|R|$) was less than 0.7 (24), which took into account only segments in which the absolute value of the statistically significant ($P < 0.05$) correlation coefficient was greater than 0.7. We determined the lag time between changes in the OCT signal slope and blood [glu] as time delay that gave the maximal correlation coefficient. For comparison with histological cuts, we used the 1-D lateral scanning mode because the 2-D mode blurred small details on the OCT images due to averaging.

The scheme of the experiments was as follows. Pigs were premedicated with telasol, 5 mg/kg im, and then they were anesthetized with 1% isoflurane by inhalation. A femoral arterial catheter was placed and was used to obtain blood samples (1 ml). Through an intravenous catheter, 0.9% saline was infused at a rate of 3–8 ml/hr to prevent dehydration. We monitored arterial saturation and heart rate with a pulse oximeter (SIMS BCI, Inc., Waukesha, WI) and blood pressure directly through the arterial catheter. Glucose (50% solution) and NaCl (7.7% solution) were injected through a femoral venous catheter or an ear vein catheter. In each blood sample, we measured [glu], [Na^+], potassium concentration [K^+], chloride concentration [Cl^-], bicarbonate concentration [HCO_3^-], urea, pH, PCO_2, total CO_2 (TCO_2), hemoglobin, and Hct. Blood analysis was performed with an i-STAT1 analyzer (i-STAT Corporation, East Windsor, NJ) that measures the analytes in one blood sample.

By design, we induced rapid large physiologically relevant acute changes in [Na^+] and [glu] to assess the response of the OCT signals. Hyperosmotic NaCl (7.7%) was infused intravenously during 8–15 mins using a digital pump at a rate of 2.4–3.8 ml/min. As a result, blood [Na^+] concentration increased rapidly from a baseline level of approximately 133–143 mM (range, 6–13 mM).

The glucose infusion was performed not earlier than 40–60 mins after the NaCl infusion. Glucose solution (50%) was injected at a rate of 2.4–3.8 ml/min for approximately 30 mins. Blood [glu] increased from approximately 80–90 mg/dl to approximately 400 mg/dl.

Our experimental sequence was designed to progressively increase our knowledge of changes in the OCT signal slope associated with changes in analyte concentrations. In our first experiment, we used one anesthetized pig to estimate the expected physiological changes in various analytes and their influences on the OCT signals. In the second experiment, we infused 80 ml of 50% glucose. In Pigs 3 and 4, we injected 60 ml of 7.7% saline. In Pigs 5 and 6, after injecting 45 ml of 7.7% saline, we injected 80 ml of 50% glucose solution. In Pigs 7 through 11, we injected 30 ml of 7.7% saline and 100 ml of 50% glucose solution. In two pigs (Pigs 12 and 13), we administered 115 ml of 50% glucose before injection of 35 ml of 7.7% saline.

To estimate reproducibility of the OCT method for blood glucose monitoring, we induced two acute changes in [glu] in two pigs. The [glu] was consequently increased by 376 mg/dl (from 69–445 mg/dl) and then by 320 mg/dl (from 153–473 mg/dl) in the first pig. In the second pig, the increase of [glu] was by 256 mg/dl (from 92–348 mg/dl) and then by 308 mg/dl (from 130–438 mg/dl).

During the experiment, the OCT device was continuously operating in the 2-D lateral scanning mode for speckle averaging. However, during individual blood sampling, we used the 1-D lateral scanning mode for comparing the OCT images with histology.

Pigs were killed at the end of the experiment under deep isoflurane anesthesia by intravenous injection of 0.4 ml/kg of saturated KCl solution. Immediately after death, the scanned area of the skin was marked using a tissue marking dye (Triangle Biomedical Sciences, Inc., Durham, NC) that is preserved during staining procedures. The marked tissue site was sectioned and stained by H&E.

Results

Comparison between H&E-stained sections was performed to identify specific layers on the OCT images (Fig. 2). Although the OCT signal slope correlated well with [glu] and [Na^+] in all pigs, the best correlations between the OCT signal slope and [glu] and [Na^+] occurred in specific depths of tissue rather than the full thickness of pig skin (Table 1). Moreover, depending on depth, the correlation coefficient of the OCT signal slope with [glu] can be positive (the OCT signal slope increased with [glu]) or negative (the OCT signal slope decreased with [glu]) due to the layered structure of skin. In one or more layers of tissue, good correlation of the OCT signal slope with blood [glu] was observed in all pigs (correlation coefficient range, –0.95 to 0.98; $|R|$, 0.88 ± 0.07). In one or more layers of tissue, the correlation of the OCT signal slope with [Na^+] was observed in 10 of 11 pigs (correlation coefficient range, –0.89 to 0.89; $|R|$, 0.78 ± 0.07). The maximal correlation between [glu] and the OCT signal slope was found at the boundary between the dermis and the hypodermis at a depth of 500–650 μm. At this depth, a strong correlation ($|R| > 0.8$) was observed in seven of 10 pigs. The OCT signal slope also correlated with blood [glu] in other skin layers, especially near the papillary-reticular junction in the dermis (five of 10 pigs) at a depth of 130–230 μm. Two pigs had strong correlations near the dermis-epidermis junction (depth, 80–130 μm). In six pigs (Pigs 8–13), the correlation was observed at several depths. The induced changes in [Na^+] before glucose injection in these pigs were from 4–7 mM.

The maximum correlation of the OCT signal slope with

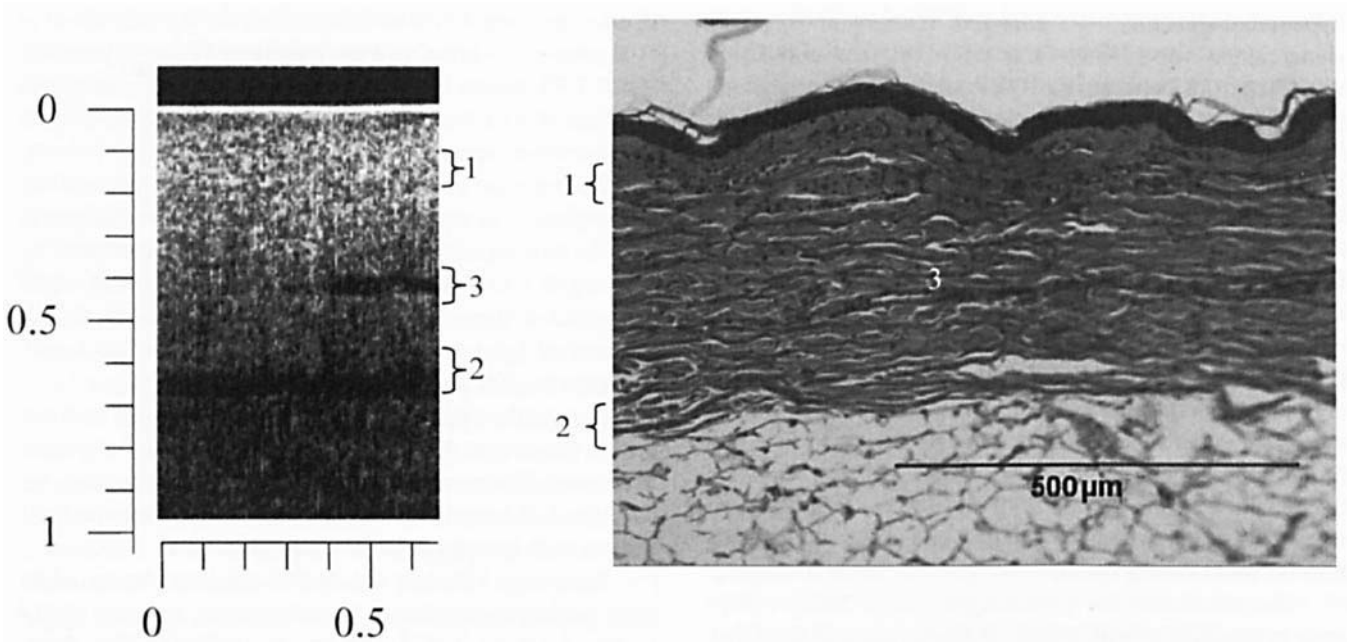

Figure 2. OCT image and histological section of pig skin (Pig 10). Points 1 and 2 on the OCT image and the histological section demonstrate the layers at which the correlation coefficients between the OCT signal slope and blood [glu] were highest in many of the pigs. Point 3 on the OCT image is most likely a blood vessel.

blood [Na^+] was also observed in separate layers. In six of nine pigs, the maximal correlation of the OCT signal slope with [Na^+] was observed in the same layers as the maximal correlation with [glu].

However, the relative changes in the OCT signal slopes induced by variation of [glu] were much greater than changes due to [Na^+] variation. The relative changes in the OCT signal slopes were calculated as the percentage of baseline and were correlated with [glu] and [Na^+] variations of 10 m*M* (180 mg/dl) (Table 1). The averaged relative [glu]-induced changes in the OCT signal slope were 5-fold greater than changes in the OCT signal slope associated with [Na^+] variation (Fig. 3). Thus, this method is sufficiently sensitive to measure blood [glu] in the physiological range of 70–570 mg/dl (range, 3.9–31.7 m*M*), as long as [Na^+] remains constant or as long as changes in the OCT signal slope caused by changes in [glu] are compensated for changes induced by [Na^+] variation.

The maximum correlation between the OCT signal slope and blood [glu] and [Na^+] was delayed (i.e., there was a lag time between changes in blood [glu] and [Na^+] and corresponding changes in the OCT signal slope). The lag time between changes in [Na^+] and changes in the OCT signal slope ranged up to 30 mins. This result was in agreement with data in the literature (3, 25). The lag time was presumably related to physiological and physical aspects of equilibration and metabolism between interstitial and intravascular systems in skin.

The sequence of individual experiments provided considerable information. In our first anesthetized pig, during 5 hrs of anesthesia, no concentration of any analyte substantially changed except [glu], which varied from 77–97 mg/dl. Those changes are well within the normal physiological range. [Na^+] variation did not exceed 3 m*M*. In the absence of substantial changes in blood concentrations of other osmolytes, we observed no correlation with the OCT signal slope.

In the second experiment, we infused only glucose and observed a strong correlation between the OCT signal slope and blood [glu] ($R = 0.82$) at a depth of 180–236 μm. This layer corresponded to the dermis-epidermis junction and had high vascularization by capillary blood vessels. The pig had unusually thick skin (>800 μm), and it was impossible to visualize the dermis-hypodermis junction, where the best correlation was observed in other pigs.

In the next four pigs (Pigs 3–6), infusion of 7.7% saline increased [Na^+] by a mean of 16 ± 4.2 m*M* (range, 11–20 m*M*) from the baseline. In Pigs 5 and 6, the correlation coefficients between the OCT signal slope and blood [glu] were 0.76 and 0.75, respectively. In Pigs 7 through 11, blood [glu] correlated more strongly with the relative OCT signal slope (correlation coefficient range, –0.95 to 0.98; $|R|$, 0.88 ± 0.08 in the four pigs). The strongest correlations were observed in several dermis layers and near the dermis-hypodermis junction. In these pigs, before glucose infusion the [Na^+] was increased by no more than 8 m*M*.

In Pigs 12 and 13, in which 50% glucose was infused before 7.7% saline, the OCT signal slopes correlated with [glu] and [Na^+] at several depths (Table 1). Correlations between the OCT signal slopes and [glu] and [Na^+] were not influenced by the order of injection (i.e., glucose before saline or saline before glucose).

Figure 4 shows typical results of experiments on reproducibility of the OCT blood glucose monitoring. In

Table 1. *R* of the OCT Signal Slopes with Various Analytes

Pig No.	[glu] Range (mg/dl)[a]	*R* for [glu] (depth range, μm)	Dermis-hypodermis junction depth (μm)	Lag time (mins)	[Na^+] range (m*M*)[b]	*R* for [Na^+] (depth range, μm)	Lag time (mins)	Δglu (% /10 m*M*)[c]	ΔNa^+ (% /10 m*M*)[d]
1	77–97 [20]	Control	450	—	128–131 [3]	—	—	—	—
2	100–325 [225]	0.82 (180–236)	595	3	127–132 [5]	Not injected	—	8.3	—
3	47–58 [11]	Not injected	500	—	132–151 [19]	0.73 (104–194)*	25	—	3.7
						0.72 (300–390)*	25		
4	58–50 [8]	Not injected	530	—	133–153 [20]	−0.81 (281–400)*	29	—	4.9
5	96–325 [229]	0.76 (98–125)	520	26	138–152 [14]	—	—	26.3	—
6	38–223 [185]	0.75 (135–225)	605	0	142–153 [11]	0.72 (488–578)	0	19.3	5.9
		0.85 (565–600)				0.74 (565–600)	7		
7	110–400 [290]	−0.9 (398–453)	500	16	130–138 [8]	−0.71 (398–453)	6	19.6	4.9
8	100–475 [375]	0.9 (594–663)	660	20	132–139 [7]	0.7 (318–387)*	0	13.6	7.2
		0.9 (318–387)		20					
		0.9 (432–502)		20					
9	60–375 [315]	0.7 (195–273)*	630	26	134–138 [4]	0.8 (507–585)*	4	44.3	13.5
		0.94 (507–585)		0					
		−0.93 (533–611)		13					
10	98–425 [327]	−0.94 (83–135)	660	1	132–138 [6]	0.89 (159–237)	13	15.3	16.9
		−0.95 (109–161)		17					
		0.77 (343–421)		5					
		0.82 (577–655)							
11	98–420 [322]	0.98 (549–601)	615	2	131–136 [5]	0.7 (100–130)*	9	23.6	11
		−0.9 (150–180)							
		0.82 (419–497)							
12	71–460 [389]	0.89 (340–430)	580	26	131–139 [8]	0.81 (340–430)	19	16	11.8
		−0.89 (460–550)				−0.76 (460–550)*			
		−0.9 (480–570)		30					
13	71–451 [380]	0.92 (350–420)	605	18	128–136 [8]	0.88 (350–420)	19	27	25
		−0.89 (395–465)		5		−0.89 (395–465)			
		0.94 (490–560)		16					
		−0.91 (530–600)		26					

[a] The difference between maximum and minimum values of [glu] variations is given in brackets.
[b] The difference between maximum and minimum values of [Na^+] variations is given in brackets.
[c] Δglu indicates variations of the OCT signal slopes from baseline induced by [glu].
[d] ΔNa^+ indicates variations of the OCT signal slopes from baseline induced by [Na^+].
* $P < 0.05$ ($P < 0.01$ for all other comparisons in the column).

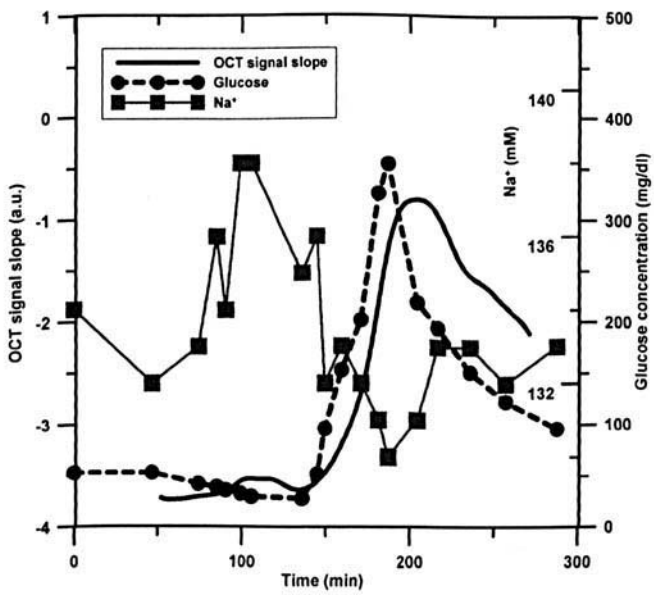

Figure 3. OCT signal slope, blood [glu], and blood [Na^+] versus time in Pig 9.

the first pig, the correlation of the OCT signal slope with [glu] was observed near the dermis-hypodermis junction (570 μm) at the depths of 480–545 μm and 505–570 μm. At the depths of 480–545 μm, the correlation coefficients between the OCT signal slope and [glu] and the lag times (T) were as follows: $R_1 = 0.92$ ($P < 0.01$), $T_1 = 8$ mins for the first peak; $R_2 = 0.91$ ($P < 0.01$), $T_2 = 8$ mins for the second peak; and $R_t = 0.78$ ($P < 0.01$), $T_t = 8$ mins for the whole experiment. At the depths of 505–570 μm, the correlation coefficients and the lag times were $R_1 = -0.95$ ($P < 0.01$), $T_1 = 8$ mins; $R_2 = -0.83$ ($P < 0.01$), $T_2 = 8$ mins; and $R_t = -0.71$ ($P < 0.01$), $T_t = 8$ mins. In this case, the relative change in the OCT signal slope with [glu] was 17% per 180 mg/dl (10 m*M*) for the first peak and 16% per 180 mg/dl for the second peak. In the second pig, the correlation was observed near the papillary-reticular junction (90 μm) and the dermis-hypodermis junction (545 μm) at the depths of 110–175 μm and 480–545 μm, respectively. At the depths of 110–175 μm, the correlation coefficients and the lag times were $R_1 = -0.77$ ($P < 0.01$), $T_1 = 11$ mins; $R_2 =$

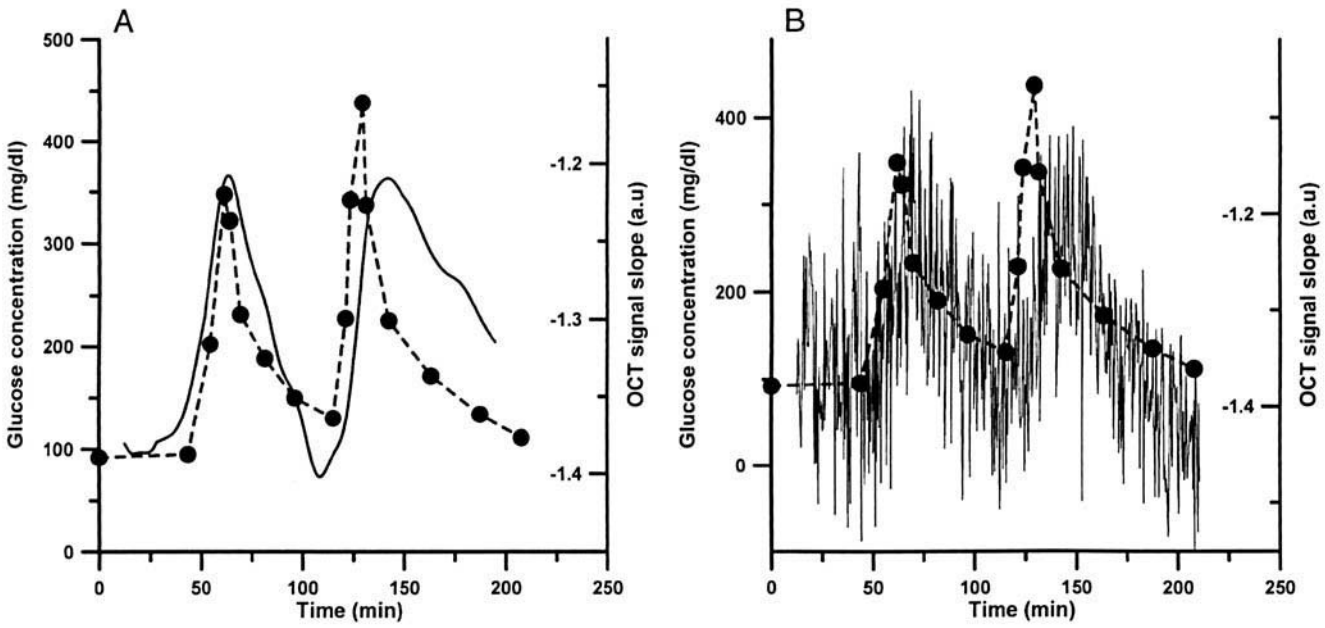

Figure 4. Filtered (A) and nonfiltered (B) OCT signal slope (solid black) and blood [glu] (dashed grey) versus time for the second pig (depth range, 480–545 μm) in the experiments on reproducibility of the OCT signal for blood glucose monitoring. During rapid changes in [glu] (glucose injections), the filtered OCT signal slope increased earlier than [glu] due to processing distortions in the slow component, while the unfiltered OCT signal slope closely follows [glu].

-0.70 ($P < 0.05$), $T_2 = 15$ mins; and $R_t = -0.66$ ($P < 0.01$), $T_t = 12$ mins. In this case, the relative change in the OCT signal slope with [glu] was 26% per 180 mg/dl for the first peak and 29% per 180 mg/dl for the second peak. At the depths of 480–545 μm, the correlation coefficients and the lag times were $R_1 = 0.86$ ($P < 0.01$), $T_1 = 2$ mins; $R_2 = 0.72$ ($P < 0.05$), $T_2 = 5$ mins; and $R_t = 0.72$ ($P < 0.01$), $T_t = 3$ mins. In this case, the relative change in the OCT signal slope with [glu] was 10% per 180 mg/dl for the first peak and 8% per 180 mg/dl for the second peak. At the other depths, the correlation of the OCT signal slope with [glu] was not observed.

In general, analytes other than [glu] and $[Na^+]$ (i.e., $[Cl^-]$, $[K^+]$, Hct, PCO_2, pH, and urea) correlated poorly with the OCT signal slope (Table 2 and Fig. 5). However, in one-half of the experiments, during infusion of NaCl, the OCT signal slope correlated with $[Cl^-]$ ($|R| = 0.7$–0.8). The correlation coefficients of the OCT signal slope with other analytes were calculated at the depths (with the corresponding lag times) at which the maximal correlation of the OCT signal slope with [glu] was observed. In the cases in which no injection of glucose was performed (Pigs 3 and 4), the correlation coefficients were calculated at the depths (with the corresponding lag times) at which the maximal correlation of the OCT signal with $[Na^+]$ was observed.

Discussion

In this study, we estimated the influences of various analytes on the OCT signal slope, although we directly altered only [glu], $[Na^+]$, and $[Cl^-]$. Our investigations demonstrated that the OCT technique is highly sensitive to changes in [glu]. However, changes in the OCT signal slope induced by changes in $[Na^+]$ within a clinically relevant range could be similar in magnitude to those induced by changes in [glu]. Previous studies reported that normal changes in $[Na^+]$ ranged 1–2 m*M* during a 24-hr interval in individual subjects (26); intersubject differences between normal individuals did not exceed 10 m*M* (27). Our data suggested that the large variation of $[Na^+]$ (138–153 m*M* after infusions in Pigs 5 and 6) caused variation of other blood osmolyte concentrations. When glucose was infused subsequent to large changes in $[Na^+]$, correlations between the OCT signal slope and [glu] were less robust. However, this clinical sequence would occur rarely, if ever. Increases in [glu] secondary to 50% glucose injection reduced $[Na^+]$, which corresponds to a clinically observed reduction in $[Na^+]$ by hyperglycemia as described in patients with diabetes (28). This phenomenon must be considered in the analysis of the influence of changes in [glu] on the OCT signal from human tissue.

Experimental variation of $[Na^+]$ that exceeded the usual physiological ranges reduced the correlation coefficient between the OCT signal slope and blood [glu]. However, the order of injection (i.e., 50% glucose before 7.7% saline or *vice versa*) did not apparently influence the sensitivity of the OCT monitoring of [glu]. In other experiments in which $[Na^+]$ variation did not exceed the usual physiological range, the correlation of the OCT signal slope with blood [glu] was sufficiently great and was observed in several skin layers. We confirmed the limited influence of high $[Na^+]$ on the sensitivity of the OCT glucose monitoring in several experiments (Pigs 7–13), when the $[Na^+]$ changed within a

Table 2. *R* of the OCT Signal Slopes with Various Analytes*

Pig No.	$[Cl^-]$ range (m*M*)	$[K^+]$ range (m*M*)	Hct range (%)	PCO_2 range (mm Hg)	pH range	Urea range (mg/dl)
1	110–116 [6]	4.3–4.9 [0.6]	19–23 [4]	55.0–60.4 [5.4]	7.356–7.380 [0.025]	8–10 [2]
2	97–100 [3]	3.9–4.6 [0.7]	20–26 [6]	60–128 [68]	7.28–7.33 [0.05]	7–8 [1]
	0.15	**0.45**	**0.12**	**0.04**	**0.19**	**0.2**
3	99–116 [7]	3.0–4.5 [1.5]	20–47 [27]	68–80 [12]	7.23–7.30 [0.07]	10–12 [2]
	−0.72	**0.33**	**0.55**	**0.36**	**0.45**	**0.46**
4	100–116 [16]	4.43–2.90 [1.53]	20–40 [20]	80–62 [18]	7.36–7.26 [0.1]	6–9 [3]
	0.78	**0.73**	**0.5**	**0.73**	**0.63**	**0.24**
5	104–118 [14]	3.5–5.0 [1.5]	17–28 [11]	75–96 [21]	7.3–7.1 [0.2]	9–13 [4]
	−0.79	**0.29**	**0.15**	**0.07**	**−0.14**	**0.24**
6	115–124 [9]	4.5–3.8 [0.7]	33–29 [4]	61–49 [12]	7.36–7.31 [0.05]	8–12 [4]
	0.81	**0.2**	**0.35**	**0.44**	**0.3**	**0.2**
7	96–108 [12]	4.4–3.6 [0.8]	18–22 [4]	50–65 [15]	7.28–7.35 [0.07]	7–10 [3]
	−0.05	**−0.45**	**−0.29**	**−0.08**	**−0.048**	**−0.59**
8	102–106 [4]	4.0–3.6 [0.4]	23–18 [5]	41–53 [12]	7.36–7.44 [008]	7–10 [3]
	−0.06	**0.29**	**0.26**	**−0.59**	**0.65**	**−0.54**
9	101–106 [5]	4.0–4.7 [0.7]	20–26 [6]	52–44 [8]	7.35–7.42 [0.07]	6–15 [9]
	−0.41	**0.31**	**0.1**	**−0.65**	**0.29**	**0.67**
10	99–107 [8]	3.6–4.4 [0.8]	22–17 [5]	60–62 [2]	7.27–7.32[0.05]	6–10 [4]
	−0.23	**0.62**	**0.48**	**−0.27**	**0.72**	**0.48**
11	100–105 [5]	4.2–3.6 [0.6]	23–16 [7]	52–50 [2]	7.35–7.3 [0.05]	4.8–6.0 [1.2]
	−0.1	**0.75**	**0.65**	**−0.02**	**−0.53**	**0.3**
12	95–105 [10]	3.6–4.4 [0.8]	18–25 [7]	50.1–62.7 [12.6]	7.28–7.36 [0.08]	6–8 [2]
	−0.13	**0.65**	**−0.26**	**0.32**	**0.4**	**0.06**
13	97–108 [11]	3.8–4.4 [0.6]	15–22 [7]	44.7–51.1 [6.4]	7.39–7.44 [0.05]	6–8 [2]
	0.72	**0.76**	**−0.8**	**−0.85**	**−0.22**	**−0.43**

*R values are in boldface type. The difference between maximum and minimum values of variation of the analytes is given in brackets.

wider range (128–138 m*M*). In these experiments, the ranges of concentrations of other analytes were smaller, and the correlation coefficients between blood [glu] and the OCT signal slopes were as high as 0.9. The relative changes induced in the OCT signal slopes by variation of [glu] ranged from 0.9–4.0 times the changes in the OCT signal slope induced by equimolar changes of $[Na^+]$, with a mean of 2.26 ± 1.15 for the eight animals studied (Pigs 6–13).

The relative changes in the OCT signal slope induced by increasing [glu] to 10 m*M* (180 mg/dl) ranged from 8%–

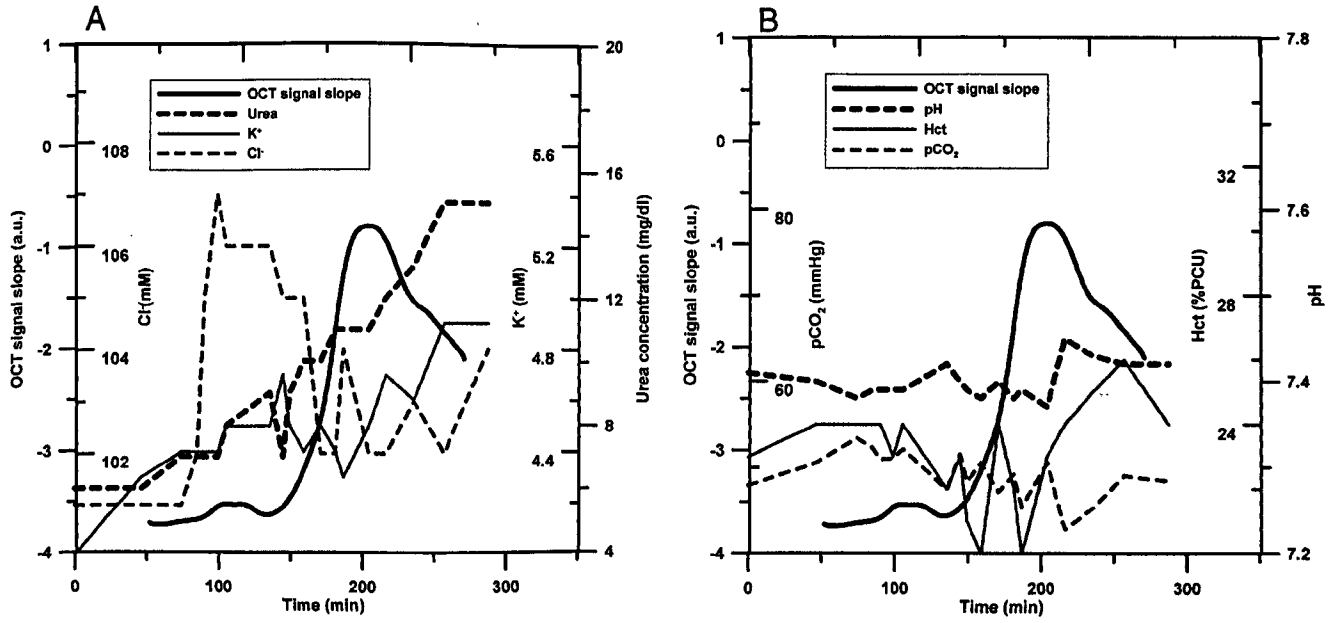

Figure 5. (A) OCT signal slope, blood $[K^+]$, blood $[Cl^-]$, and blood urea concentration versus time in Pig 9. (B) OCT signal slope, pH, PCO_2, and Hct versus time in Pig 9.

44%, in comparison with 4.9%–25% changes induced by changing [Na^+] by 10 m*M*. Assuming that diurnal variations of [Na^+] usually averaged 1–2 m*M* and that clinically important variations in [glu] would exceed 30 mg/dl, we conclude that precise monitoring of [glu] using OCT may require correction of [glu] estimates for changes in [Na^+]. The changes in the OCT signal slope per 1 m*M* of [glu] were different, which indicated the necessity of the OCT system calibration for each patient (a limitation factor for OCT-based glucose monitoring).

Secondary changes in [K^+], Hct, PCO_2, pH, and urea that were produced by infusion of 7.7% saline or 50% glucose did not significantly influence the sensitivity of the OCT [glu] monitoring. Alterations of [Cl^-], which were primarily changed by infusion of 7.7% saline, had less influence than [glu] or [Na^+]. During 7.7% saline injections, [Cl^-] correlated with the OCT signal slopes in five of 12 experiments. Only in one experiment (Pig 13) was there a correlation of the OCT signal slope and biochemical variables other than [glu], [Na^+], and [Cl^-].

Despite the promising results obtained with the OCT method of monitoring [glu], some technical difficulties must be resolved. Most important, the strong correlation coefficients ($|R| > 0.7$) between the OCT signal slopes and [glu] were observed only at specific layers, which varied among pigs, and the OCT signal slopes could correlate either positively or negatively with changes in [glu]. The principles governing these correlations must be determined.

Most often, the strongest correlations between the OCT signal slopes and [glu] were observed in two skin regions: near the papillary-reticular border of the dermis and at the dermis-hypodermis junction. The high vascularity of these regions could explain the better and more rapid equilibration between blood [glu] and interstitial [glu]. However, the major mechanism underlying the correlation between the OCT signal slopes and blood osmolytes concentration is controversial. Two hypotheses have been advanced to explain the correlation. The first hypothesis is based on the fact that changes in osmolyte concentration result in aligning of the mismatch of refractive indices of extracellular and intracellular components and therefore decrease the scattering coefficient of tissue (3, 29). This hypothesis was used to explain the correlation between the OCT signal slope and [glu] in a previous pilot study (5). The second hypothesis is based on morphological changes in tissue. Possibly, the osmotic influence of changing [glu] causes shrinkage or expansion of the dermis. Therefore, the shift of tissue layers (collagen fibers) may result in changes in the OCT signal slope with [glu] at a certain depth. In addition, the OCT signal slope may be affected by dehydration, leading to more dense packing of scattering constituents, for example, collagen fibers (30, 31). The similar [glu]-induced osmotic effect producing reabsorption of fluids in the proximal tubule was shown by Weinstein et al (32). We directly measured the shrinkage of dermis using the OCT images obtained in the 2-D lateral scanning mode and found a strong correlation ($|R| > 0.7$) in 75% of experiments between dermis thickness and variation of blood [glu]. These data indicate that the [glu]-induced osmotic effects are significant.

The other technical problem confronting noninvasive monitoring of blood [glu] by OCT is the substantial lag time between changes in the OCT signal slope and blood [glu]. Using OCT, we measured changes in blood [glu] indirectly by detecting the influence of [glu]-induced changes in interstitial fluid on the skin optical properties. The lag time was as long as 30 mins and could reflect changes in skin hydration as interstitial fluid concentrations equilibrated with intravascular fluid concentrations. Under acute changes of [glu], the interaction and distribution of fluids (glucose and interstitial fluids) in tissue are described by the mass transfer equation. Therefore, the lag time is determined by the mass transfer resistance from the blood to subcutaneous regions (25). The equilibration of [glu] between these fluids after increasing blood [glu] took approximately 15 mins in humans (3). The morphological reorganization of dermis could also require time. Whichever mechanism is involved, the problem of reducing the lag time for noninvasive biosensors demands further consideration.

Results of preliminary experiments on reproducibility of blood glucose monitoring confirmed that the best correlation of the OCT signal slope with [glu] was observed near the dermis-hypodermis junction in most cases. The amplitude difference between [glu]-induced relative changes in the OCT signal slope did not exceed 10% for the first peak and the second peak, and the difference in the lag time did not exceed 4 mins for the papillary-reticular junction and 3 mins for the dermis-hypodermis junction. It should be noted that, based on reproducibility investigations, the difference in the amplitudes and the lag times between these two peaks decreased with increase of the correlation coefficient. The difference in these parameters is caused by the residual speckle noise, motion artifacts, and changes in the morphofunctional state of skin during the measurements not induced by [glu]. In the second animal, at the depth of 110–175 μm, the total correlation coefficient of the OCT signal slope with [glu] was less than 0.7, which was most likely due to the difference between the lag times for the two peaks of [glu].

The relative amplitude of [glu]-induced changes in the OCT signal slope and the lag times varied between animals and were depth-dependent. Therefore, one would need to calibrate the OCT system for each patient and for different depths in a particular patient.

To reduce the influence of speckle noise to acceptable levels, we averaged 1800 independent A-scans that required 30 secs. For anesthetized animals, this time is short enough to avoid motion artifacts, but in clinical conditions in which the motion artifacts are more significant, the scanning time should be reduced. In our experiments, we used a time domain OCT system, but faster frequency domain systems with 16,000–18,000 A-scans/sec are available (33, 34).

Using a high-speed frequency domain system, the scanning time for 1800 A-scans would take about 0.1 sec, which is acceptable for *in vivo* measurements in nonanesthetized subjects.

In this article, we demonstrate the sensitivity of the OCT method to changes in [glu], [Na^+], and concentrations of other osmolytes. We obtained the following results: (i) The sensitivity of the OCT signal slope was 2.26 ± 1.15 greater for blood [glu] than for [Na^+] in the physiological range of these osmolytes. (ii) Correlations between the OCT signal slope with [glu] and [Na^+] were observed when the OCT signal slopes were calculated in specific layers of skin but not when calculated from full skin thickness. Therefore, OCT as a high-resolution technique allowing layer-by-layer probing is a promising method for noninvasive glucose monitoring. (iii) The maximum correlation of the OCT signal slope with blood [glu] was observed near the border of papillary and reticular layers and near the dermis-hypodermis junction. Correlations of the OCT signal slopes with [Na^+] were observed in the same layers. (iv) The experiments on reproducibility of the OCT monitoring of [glu] showed that the amplitude of [glu]-induced changes in the OCT signal slope and the lag time varied insignificantly at the fixed depth. Consequently, we suggest that calibration of the OCT system at a specific depth is possible, but it should be performed for each subject. (v) The osmolytes [K^+], [HCO_3^-], urea, pH, and PCO_2 did not influence the OCT signal slope, although in some animals [Cl^-] correlated with the OCT signal slope during infusion of NaCl.

1. National Institute of Diabetes and Digestive and Kidney Diseases. National Diabetes Information Clearinghouse: Diabetes Overview. Available at: http://diabetes.niddk.nih.gov/dm/pubs/overview/. Accessed June 11, 2006.
2. Khalil OS. Spectroscopic and clinical aspects of noninvasive glucose measurements. Clin Chem 45:165–177, 1999.
3. Koschinsky T, Heinemann L. Sensors for glucose monitoring: technical and clinical aspects. Diabetes Metab Res Rev 17:113–123, 2001.
4. Hull EL, Ediger MN, Unione AHT, Deemer EK, Stroman ML, Baynes JW. Noninvasive, optical detection of diabetes: model studies with porcine skin. Opt Express 12:4496–4510, 2004.
5. Esenaliev RO, Larin KV, Larina IV, Motamedi M. Noninvasive monitoring of glucose concentration with optical coherence tomography. Opt Lett 26:992–994, 2001.
6. Larin KV, Eledrisi MS, Motamedi M, Esenaliev RO. Noninvasive blood glucose monitoring with optical coherence tomography: a pilot study in human subjects. Diabetes Care 25:2263–2267, 2002.
7. Larin KV, Motamedi M, Ashitkov TV, Esenaliev RO. Specificity of noninvasive blood glucose sensing using optical coherence tomography technique: a pilot study. Phys Med Biol 48:1371–1390, 2003.
8. Huang D, Wang J, Lin CP, Schuman JS, Stinson WG, Chang W, Hee MR, Flotte T, Gregory K, Puliafito CA, Fujimoto JG. Optical coherence tomography. Science 254:1178–1181, 1991.
9. Izatt JA, Swanson EA, Hee MR, Huang D, Schuman J, Lin CP, Puliafito CA, Fujimoto JG. Quantitative assessment of cataract development with optical coherence domain reflectometry and optical coherence tomography (abstract). Invest Ophthalmol 33:1300, 1992.
10. Gladkova ND, Petrova GA, Nikulin NK, Radenska-Lopovok SG, Snopova LB, Chumakov YP, Nasonova VA, Gelikonov VM, Gelikonov GV, Kuranov RV, Sergeev AM, Feldchtein FI. *In vivo* optical coherence tomography imaging of human skin: norm and pathology. Skin Res Technol 6:6–16, 2000.
11. Pan Y, Lavelle JP, Bastacky SI, Meyers S, Pirtskhalaishvili G, Zeidel ML, Farkas DL. Detection of tumorigenesis in rat bladders with optical coherence tomography. Med Phys 28:2432–2440, 2001.
12. Xie TQ, Zeidel ML, Pan YT. Detection of tumorigenesis in urinary bladder with optical coherence tomography: optical characterization of morphological changes. Opt Express 10:1431–1443, 2002.
13. Sergeev AM, Gelikonov VM, Gelikonov GV, Feldchtein FI, Kuranov RV, Gladkova ND, Shakhova NM, Snopova LB, Shakhov AV, Kuznetzova IA, Denisenko AN, Pochinko VV, Chumakov YP, Streltzova OS. *In vivo* endoscopic OCT imaging of precancer and cancer states of human mucosa. Opt Express 1:432–440, 1997.
14. Kamensky V, Feldchtein F, Gelikonov V, Snopova L, Muraviov S, Malyshev A, Bityurin N, Sergeev A. *In situ* monitoring of laser modification process in human cataractous lens and porcine cornea using coherence tomography. J Biomed Opt 4:137–143, 1999.
15. Hendriks FM, Brokken D, Oomens CW, Baaijens FPT. Influence of hydration and experimental length scale on the mechanical response of human skin *in vivo*, using optical coherence tomography. Skin Res Technol 10:231–241, 2004.
16. Pierce MC, Sheridan RL, Park BH, Cense B, de Boer JF. Collagen denaturation can be quantified in burned human skin using polarization-sensitive optical coherence tomography. Burns 30:511–517, 2004.
17. Choi B, Milner TE, Kim JH, Goodman JN, Vargas G, Aguilar G, Nelson JS. Use of optical coherence tomography to monitor biological tissue freezing during cryosurgery. J Biomed Opt 9:282–286, 2004.
18. Sapozhnikova VV, Kamensky VA, Kuranov RV, Kutis I, Snopova LB, Myakov AV. *In vivo* visualization of *Tradescantia* leaf tissue and monitoring the physiological and morphological states under different water supply conditions using optical coherence tomography. Planta 219:601–609, 2004.
19. Tuchin V. Optical clearing of tissue and blood using immersion method. J Phys D Appl Phys 38:2497–2518, 2005.
20. Tuchin V. Optical immersion as a new tool to control optical properties of tissue and blood. Laser Physics 15:1109–1136, 2005.
21. Van den Berghe G, Wouters P, Weekers F, Verwaest C, Bruyninckx F, Schetz M, Vlasselaers D, Ferdinande P, Lauwers P, Bouillon R. Intensive insulin therapy in critically ill patients. N Engl J Med 345: 1359–1367, 2001.
22. Larin KV, Akkin T, Esenaliev RO, Motamedi M, Milner TE. Phase-sensitive optical low-coherence reflectometry for the detection of analyte concentrations. Appl Opt 43:3408–3414, 2004.
23. Kholodnykh AI, Petrova IY, Larin KV, Motamedi M, Esenaliev RO. Precision of measurement of tissue optical properties with optical coherence tomography. Appl Opt 42:3027–3037, 2003.
24. Munro BH. Correlation. In: Statistical Methods for Health Care Research. Philadelphia: Lippincott Williams & Wilkins, pp239–258, 2005.
25. Schmidtke DW, Freeland AC, Heller A, Bonnecaze RT. Measurements and modeling of the transient difference between blood and subcutaneous glucose concentration in the rat after injection of insulin. Proc Natl Acad Sci U S A 95:294–299, 1998.
26. Guyton AC. Textbook of Medical Physiology. Philadelphia: WB Saunders, pp435–443, 1981.
27. Amede FJ, James KA, Michelis MF, Gleim GW. Changes in serum sodium, sodium balance, water balance, and plasma hormone levels as the result of pelvic surgery in women. Int Urol Nephrol 34:545–550, 2002.
28. Hillier TA, Abbott RD, Barrett EJ. Hyponatremia: evaluating the correction factor for hyperglycemia. Am J Med 106:399–403, 1999.
29. Maier JS, Walker SA, Fantini S, Franceschini MA, Gratton E. Possible correlation between blood glucose concentration and the reduced scattering coefficient of tissues in the near infrared. Opt Lett 19:2062–2064, 1994.

30. Khlebtsov NG, Maksimova IL, Tuchin VV, Wang L. Introduction to light scattering by biological object. In: Tuchin VV, Ed. Handbook of Optical Biomedical Diagnostics. Bellingham, WA: SPIE Press, Vol PM 107:pp31–167, 2002.
31. Wang RK, Tuchin VV. Optical coherence tomography: light scattering and imaging enhancement. In: Tuchin VV, Ed. Coherent-Domain Optical Methods: Biomedical Diagnostics, Environmental and Material Science. Boston: Kluwer Academic Publishers, Vol 2:pp3–60, 2004.
32. Weinstein SW, Klose R, Szyjewicz J, Moore L. Evidence for an osmotic effect of glucose in the *in vivo* rat proximal tubule. Pflugers Arch 394:320–328, 1982.
33. Park BH, Pierce MC, Cense B, Yun SH, Mujat M, Tearney GJ, Bouma BE, de Boer JF. Real-time fiber-based multi-functional spectral-domain optical coherence tomography at 1.3 μm. Opt Express 13:3931–3944, 2005.
34. Wojtkowski M, Srinivasan VJ, Ko TH, Fujimoto JG, Kowalczyk A, Duker JS. Ultrahigh-resolution, high-speed, Fourier domain optical coherence tomography and methods for dispersion compensation. Opt Express 12:2404–2422, 2004.